Effects of surface/interface stress on phonon properties and thermal conductivity in AlN/GaN/AlN heterostructural nanofilms

Siyang Zhang[1], Xiaoya Tang[1], Haihui Ruan[2], Linli Zhu[1*]

[1]Department of Engineering Mechanics, and Key Laboratory of Soft Machines and Smart Devices of Zhejiang Province, Zhejiang University, Hangzhou 310027, China

[2]Department of Mechanical Engineering, The Hong Kong Polytechnic University, Hong Kong, China

Abstract

The effect of surface/interface stress on phonon properties and thermal conductivity of GaN-based heterostructural nanofilms was theoretically investigated through the involvement of stress-dependent elastic modulus of nanostructures. The elastic model was used to quantitatively describe the spatially confined phonons in a GaN-based nanofilm under surface/interface stresses. The relationship between surface/interface stress and phonon thermal conductivity was further calculated for different phonon modes. Numerical results show that the positive (negative) surface/interface stress increases (decreases) the phonon energy and phonon group velocity while decreases (increases) the phonon density of state. With the increase of surface/interface stress, the phonon thermal conductivity of a nanofilm increases in SH mode but decreases in AS and SA modes. The surface/interface stress can also alter the temperature dependence of phonon thermal conductivity in heterostructural

* Author to whom correspondence should be addressed; electronic mail: llzhu@zju.edu.cn (Linli Zhu).

nanofilms. These simulation results will contribute to the analysis of heat transport in GaN-based heterostructural nanostructures and provide the theoretical support for the thermal performance design and optimization in GaN-based electronic devices.

Keywords: AlN/GaN/AlN nanofilms; Surface/interface stress; Effective elastic modulus; Phonon properties; Phonon thermal conductivity; Elastic model.

1 Introduction

The change of the bonding mode of surface atoms gives rise to electron redistribution and surface stress [1-4]. As a result, the surface energy and elasticity differ from those of the bulk. Because the thickness of surface layer is usually only of several atoms, the influence of surface layer on the overall mechanical behaviors is negligible if the concerned material is in micrometer scale and above. However, with a geometric dimension reduces into nanoscale, the occupancy of surface layer in the whole volume of a material increases rapidly, leading to the necessity to consider the influence of surface energy/stress. Besides the well-studied influence on mechanical properties [5-9], the surface energy/stress can also alter thermal, electrical, magnetic and optical properties [10-12]. Because semiconductor nanostructures have been widely used in micro/nanoelectronic devices such as transistors and sensors [13-17], it is of great significance to explore the effect of surface energy/stress on the physical properties in semiconductor nanostructures for the design and reliability analysis of micro/nano devices.

A lot of work have been carried out to investigate the effects of surface/interface energy and surface/interface stress on the mechanical and physical properties of nanostructures [6, 7, 18-21]. The first systematic description of the surface mechanical behavior of solids was developed by Gurtin and Murdoch [22] in the framework of continuum mechanics, which has been widely used in the analysis of the size-dependent elastic properties of nanostructures [23-26]. **For example, Karimi et al. used the Gurtin-Murdoch's theory to analyze the surface and nonlocal effects on the vibration and buckling behaviors in double/multi-layers nanoplates including the magneto-electro-thermo-elastic nanoplates [21, 27-30].** When there is no external loading, the nanostructure could be subjected to the residual stress induced by the surface tension. Wang *et al.* demonstrated that the surface tension and related residual stress could affect the elastic modulus of the heterogeneous nanostructure [31]. Miller *et al*. found that some important physical properties of nanostructures such as elastic modulus, melting point and yield strength, are size-dependent, and the surface/interface energy can be introduced into the total strain energy of nanostructures to explain the size dependence of mechanical properties [32]. Liangruksa *et al.* [33] used a continuum mechanics model to study the relationship between surface stress and phonon properties of Si nanowires and found that the surface stress significantly affected the phonon dispersion relationship and the lattice thermal conductivity. It has also been proved in both simulations and experiments that the surface roughness of Si nanowires can significantly affect the phonon mean free path and lattice thermal conductivity [34, 35]. Furthermore, Zhu

and his coworkers applied an elastic model to investigate the effects of stress fields on phonon properties and phonon thermal conductivity of nanostructures, in which the acoustoelastic and surface/interface stress effects were involved [36-39]. Since semiconductor nanostructures in actual micro/nanoelectronic devices are often heterostructural nanofilms [40-44], it is necessary to provide an insight into the phonon properties and thermal properties of heterostructural nanofilms. For instance, Zou *et al.* modeled lattice thermal conductivity in AlN/GaN/AlN heterostructural nanofilms considering the effects of partial phonon spatial confinement [45]. **These studies have demonstrated that surface/interface properties significantly influence the mechanical and physical properties of the heterostructural nanostructures.** However, their influence on phonon properties and thermal conductivity of semiconductor heterostructural nanofilms is rarely studied so far.

In this work, the phonon properties and phonon thermal conductivity of GaN-based heterostructural nanofilms are calculated by considering the effects of quantum confinement and the surface/interface stress. The effective elastic moduli of each layer in a heterostructure are obtained in the framework of continuum mechanics considering the surface energy/surface stress effects. **Such an elastic model is applied to describe the confined phonons for shear (SH) mode, dilatational (SA) mode and flexural (AS) mode in heterostructural nanofilms. Numerical results show that the surface /interface stress can significantly influence the phonon properties and phonon thermal conductivity in GaN-based heterostructural nanofilms. The positive (negative) surface/interface stresses increase (decrease)**

the phonon energy and phonon group velocity while decrease (increase) the phonon density of state for SH mode of phonons. With increasing the surface/interface stresses from negative value to positve one, the phonon thermal conductivity for SH mode is enhanced significantly while that for AS mode and AS mode is weakened slightly in GaN-based heterostructural nanofilms. These results will provide the theoretical support for precisely predicting the phonon and thermal properties in heterogeneous nanostructures and controlling these properties through surface/interface engineering.

2 Theoretical model

2.1 Continuum elastic model of confined phonons in heterostructural nanofilms

A three-layered nanofilm composed of AlN, GaN and AlN is studied as an example of GaN-based heterostructural nanofilm. The acoustic phonons of spatially confined nanofilms can be well described by the continuous elastic model [46-49]. It is assumed that each layer in the heterostructural film is isotropic in the natural state, as shown in Fig. 1. Then, the vibration control equation of the heterostructural nanofilms can be expressed as

$$\rho(x_3)\frac{\partial^2 u_i}{\partial t^2}=\frac{\partial}{\partial x_j}(\bar{C}_{ijkl}(x_3)\frac{\partial u_k}{\partial x_l}), \quad (1)$$

where ρ, $\bar{C}_{ijkl}$, and u_i are the density, elastic modulus tensor and the displacement tensor, respectively, the subscripts *i, j, k, l* are the indices of Cartesian coordinate axes. x_1 and x_2 represent the plane directions of the thin film as shown in Fig.1; and x_3 represents the thickness direction of the thin film, which is also the hexagonal axis

direction of AlN and GaN crystals in the film. Since the density and elastic moduli of GaN are different from those of AlN, these parameters become the function of x_3 in a heterostructural film.

Due to the heterogeneity of GaN-based nanofilms, the variations of density and elastic modulus tensor with the thickness of the film are given by:

$$\rho(x_3)=\begin{cases}\rho_{AlN}, -\frac{t_{GaN}}{2}-t_{AlN}\le x_3\le -\frac{t_{GaN}}{2}\\ \rho_{GaN}, -\frac{t_{GaN}}{2}\le x_3\le \frac{t_{GaN}}{2}\\ \rho_{AlN}, \frac{t_{GaN}}{2}\le x_3\le \frac{t_{GaN}}{2}+t_{AlN}\end{cases}, \bar{C}_{ij}(x_3)=\begin{cases}\bar{C}_{ijAlN}, -\frac{t_{GaN}}{2}-t_{AlN}\le x_3\le -\frac{t_{GaN}}{2}\\ \bar{C}_{ijGaN}, -\frac{t_{GaN}}{2}\le x_3\le \frac{t_{GaN}}{2}\\ \bar{C}_{ijAlN}, \frac{t_{GaN}}{2}\le x_3\le \frac{t_{GaN}}{2}+t_{AlN}\end{cases}, \quad (2)$$

where $\bar{C}_{ij}$ is the effective elastic modulus tensor involving the influence of surface/interface residual stresses, which will be detailed in Section 2.2. Here, we have used the Voigt notation to contract the indices, i.e., $(iijj)\rightarrow(ij)$, $(12)\rightarrow(6)$, $(13)\rightarrow(5)$, and $(23)\rightarrow(4)$. The solution of displacement field of the membrane vibration satisfying Eq. (1) is obtained as:

$$u=\bar{u}(x_3)\exp[i(\omega t-q\cdot x_1)], \quad (3)$$

where ω, q, and $\bar{u}$ are the phonon frequency, wave vector and amplitude of the displacement vector, respectively. Substituting Eq. (3) into Eq. (1) leads to:

$$\mathbf{D}\bar{u}(x_3)=-\rho\omega^2\bar{u}(x_3), \quad (4)$$

where

$$\mathbf{D}=\begin{bmatrix} \bar{C}_{44}\frac{d^2}{dx_3^2}-C_{11}q^2+\frac{d\bar{C}_{44}}{dx_3}\frac{d}{dx_3} & 0 & -iq(\bar{C}_{13}+\bar{C}_{44})\frac{d}{dx_3}-iq\frac{d\bar{C}_{44}}{dx_3} \\ 0 & \bar{C}_{44}\frac{\partial^2}{\partial x_3^2}-\bar{C}_{66}q^2+\frac{d\bar{C}_{44}}{dx_3}\frac{d}{dx_3} & 0 \\ -iq(\bar{C}_{13}+\bar{C}_{44})\frac{d}{dx_3}-iq\frac{d\bar{C}_{13}}{dx_3} & 0 & \bar{C}_{33}\frac{d^2}{dx_3^2}-\bar{C}_{44}q^2+\frac{d\bar{C}_{33}}{dx_3}\frac{d}{dx_3} \end{bmatrix}. \quad (5)$$

The boundary condition is

$$x_1=\pm\frac{H}{2},\sigma_{13}=\sigma_{23}=\sigma_{33}=0. \quad (6)$$

For the shear (SH) mode, the film displacement form is $\bar{u}=(0,u_2,0)$, and the eigen equation satisfy:

$$\bar{C}_{44}(x_3)\frac{d^2\bar{u}_2}{dx_3^2}+(\rho(x_3)\omega^2-\bar{C}_{66}(x_3)q^2)\bar{u}_2+\frac{d\bar{C}_{44}}{dx_3}\frac{d\bar{u}_2}{dx_3}=0. \quad (7)$$

For the dilatational (SA) mode and flexural (AS) mode, $\bar{u}=(u_1,0,u_3)$, the eigen equations are given as follows:

$$\begin{cases} \bar{C}_{44}(x_3)\frac{d^2\bar{u}_1}{dx_3^2}-iq(\bar{C}_{13}(x_3)+\bar{C}_{44}(x_3))\frac{d\bar{u}_3}{dx_3}+(\rho(x_3)\omega^2-\bar{C}_{11}(x_3)q^2)\bar{u}_1 \\ \qquad +\frac{d\bar{C}_{44}}{dx_3}\frac{d\bar{u}_1}{dx_3}-iq\frac{d\bar{C}_{44}}{dx_3}\bar{u}_3=0 \\ \bar{C}_{33}(x_3)\frac{d^2\bar{u}_3}{dx_3^2}-iq(\bar{C}_{13}(x_3)+\bar{C}_{44}(x_3))\frac{d\bar{u}_1}{dx_3}+(\rho(x_3)\omega^2-\bar{C}_{44}(x_3)q^2)\bar{u}_3 \\ \qquad +\frac{d\bar{C}_{33}}{dx_3}\frac{d\bar{u}_3}{dx_3}-iq\frac{d\bar{C}_{13}}{dx_3}\bar{u}_1=0 \end{cases}. \quad (8)$$

With the boundary conditions and the elastic modulus tensors of GaN and AlN layers, the phonon dispersion relation of SH, SA and AS modes can be numerically solved.

2.2 Effective elastic modulus in each layer of heterostructural nanofilm

Usually, the volume of surface layer is much smaller than the total volume of a

structure, hence the surface energy is often neglected in traditional continuum mechanics. However, the surface energy has a significant impact on the elastic properties of nanostructures due to the significant volume ratio of surface layer. Therefore, the effective elastic modulus of a nanostructure can be derived by involving the surface energy into the total strain energy in the continuum mechanical framework [5, 50, 51]. The total strain energy of a nanostructure consists of the bulk strain energy U_{bulk} and the surface energy $U_{surface}$, expressed as

$$\begin{aligned} U &= U_{bulk} + U_{surface} \\ &= \frac{2V_0}{H_0}\Gamma_{ij}\varepsilon_{ij} + \frac{V_0}{2}(C_{ijkl} + \frac{2}{H_0}Q_{ijkl})\varepsilon_{ij}\varepsilon_{kl} + \frac{V_0}{6}(C^{(3)}_{ijklmn} + \frac{2}{H_0}P_{ijklmn})\varepsilon_{ij}\varepsilon_{kl}\varepsilon_{mn}, \end{aligned} \tag{9}$$

where C_{ijkl} and $C^{(3)}_{ijklmn}$ are the second-order and third-order elastic constants of a crystalline material, respectively, Γ_{ij} is related to the residual surface stress $\Gamma^{(1)}_{\alpha\beta}$, Q_{ijkl} and P_{ijklmn} are related to the surface elastic constant tensors $\Gamma^{(2)}_{\alpha\beta\kappa\lambda}$ and $\Gamma^{(3)}_{\alpha\beta\kappa\lambda\gamma\eta}$, respectively, H_0 refers to the thickness of nanofilm, V_0 is the volume of the film, and ε_{ij} is the strain tensor. Then, the effective elastic modulus of a nanofilm can be expressed as [5]

$$\bar{C}_{ijkl} = \frac{\partial^2 U}{V_0 \partial\varepsilon_{ij}\partial\varepsilon_{kl}} \approx C_{ijkl} + \frac{2}{H_0}(Q_{ijkl} + C^{(3)}_{ijklmn}M_{mnpq}\Gamma_{ij}), \tag{10}$$

where $M_{mnpq} = C^{-1}_{ijkl}$ represents the compliance tensor of a crystalline material. This effective elastic modulus tensor can be simplified as follows:

$$\bar{C}_{11} = C_{11} + \frac{2}{H_0}\left[(K^s + \mu^s) + \Gamma_{11}\eta(\frac{2C_{112}}{C_{11}} - \frac{C_{111}+C_{112}}{C_{12}})\right]$$
$$\bar{C}_{33} = C_{11} + \frac{4\Gamma_{11}\eta}{H_0}(\frac{C_{111}}{C_{11}} - \frac{C_{112}}{C_{12}}), \bar{C}_{13} = C_{12} + \frac{2\Gamma_{11}\eta}{H_0}(\frac{2C_{112}}{C_{11}} - \frac{C_{123}+C_{112}}{C_{12}})$$
$$\bar{C}_{12} = C_{12} + \frac{2}{H_0}\left[(K^s - \mu^s) + 2\Gamma_{11}\eta(\frac{C_{123}}{C_{11}} - \frac{C_{112}}{C_{12}})\right] \quad , (11)$$
$$\bar{C}_{44} = C_{44} + \frac{2\Gamma_{11}\eta}{H_0}\left[\frac{2C_{155}}{C_{11}} - \frac{C_{144}+C_{155}}{C_{12}}\right], \bar{C}_{66} = C_{44} + \frac{2}{H_0}\left[\mu^s + 2\Gamma_{11}\eta(\frac{C_{144}}{C_{11}} - \frac{C_{155}}{C_{12}})\right]$$

where $\eta = C_{11}C_{12}/(C_{11}+2C_{12})(C_{11}-C_{12})$, $\Gamma_{11} = \Gamma_{11}^{(1)}$ is the residual stress on the surface. K^S and μ^S are the surface bulk and shear moduli, respectively, which are related to $\Gamma_{\alpha\beta\kappa\lambda}^{(2)}$.

For a heterostructural nanofilm consisting of two AlN layers and one GaN layer as shown in Fig.1, one can assume for simplicity that such a heterostructural nanofilm is a symmetrical structure. It means that the surface energy/stresses at top and bottom layers are identical, and the interfacial energy/stresses at the two GaN-AlN interfaces are also the same. In order to derive the effective elastic modulus of each layer in the heterostructural nanofilm, suppose that the interfacial energy between GaN and AlN can be expressed as

$$U_{interface} = U_{AlN}^S + U_{0GaN}^S, \quad (12)$$

where U_{AlN}^S is the surface energy of a AlN layer, and U_{0GaN}^S is the effective surface/interface energy of the GaN layer. Then, the GaN-based heterostructural nanofilm can be separated into two AlN layers with the surface energy of U_{AlN}^S and one GaN layer with the surface energy of U_{0GaN}^S. Thereby, the total strain energy of AlN layer and GaN layer can be written respectively as

$$U_{AlN} = U_{AlN}^{bulk} + U_{AlN}^S, \quad (13)$$

and

$$U_{GaN} = U_{GaN}^{bulk} + U_{0GaN}^{S}. \tag{14}$$

Here, the energy U_{AlN}^{S} involves the surface stress at the top and bottom surfaces, and the energy U_{0GaN}^{S} includes the effective interface stress for the interface between GaN layer and AlN layer. Substituting Eqs. (13) and (14) into Eq. (10), the effective elastic modulus of AlN layer and GaN layer can be expressed as

$$\begin{cases} \bar{C}_{ijkl}^{\mathrm{AlN}} = C_{ijkl}^{\mathrm{AlN}} + \dfrac{2}{H_{\mathrm{AlN}}}(Q_{ijkl}^{\mathrm{AlN}} + C_{ijklmn}^{(3)\mathrm{AlN}} M_{mnpq}^{\mathrm{AlN}} \Gamma_{ij}^{\mathrm{AlN}}) \\ \bar{C}_{ijkl}^{\mathrm{GaN}} = C_{ijkl}^{\mathrm{GaN}} + \dfrac{2}{H_{\mathrm{GaN}}}(Q_{ijkl}^{\mathrm{GaN}} + C_{ijklmn}^{(3)\mathrm{GaN}} M_{mnpq}^{\mathrm{GaN}} \Gamma_{ij}^{0\mathrm{GaN}}) \end{cases}. \tag{15}$$

Let $T_{\mathrm{sf}} = \Gamma_{11}^{\mathrm{AlN}}$ and $T_{\mathrm{if}} = \Gamma_{11}^{\mathrm{GaN}}$ represent the surface stress of AlN layer and AlN-GaN interfacial stresses, respectively. Combining Eqs. (11) and (15) with the Eqs. (6)-(8), one can analyze the influence of surface/interface stress on the phonon properties of a GaN-based heterostructural nanofilm.

2.3 Phonon thermal conductivity of heterostructural nanofilms

Phonon thermal conductivity is one of the important physical properties of semiconductor materials. According to the elastic model described in subsection 2.2, one can obtain the phonon dispersion relations for different modes of an AlN/GaN/AlN heterostructural nanofilm by using the finite difference method. Then, the phonon group velocity and phonon density of state can further be determined. The phonon group velocity is defined as

$$v_n(q) = \frac{d\omega_n(q)}{dq}. \tag{16}$$

The subscript n is the quantum number of the mode with a given polarization direction. For a spatially confined nanofilm, $n = H/a$, where a is the lattice constant. The phonon density of state (DOS) is defined as the total number of phonon mode number per unit volume in a unit frequency range, which could be expressed for a nanofilm as

$$f_n^{SA,AS,SH}(\omega) = \frac{1}{H}\left[\frac{1}{2\pi} q_n^{SA,AS,SH}(\omega) \frac{1}{v_n^{SA,AS,SH}}\right]. \tag{17}$$

The DOS for different modes (SA, AS, SH) can be calculated respectively, so that the total density of state is summed by

$$F(\omega) = \sum\nolimits_n f_n(\omega) \cdot \tag{18}$$

Heat flow under small temperature gradient ∇T can be expressed as:

$$J = -\sum_{q,n}^{N} (N_{q,n}^0 - N_{q,n}) \hbar \omega_n(q) v_n(q), \tag{19}$$

where $N_{q,n}$ and $N_{q,n}^0$ represent the non-equilibrium phonon distribution and the equilibrium phonon that conforms to Bose-Einstein distribution, respectively. Using the steady-state Boltazmann equation [45]:

$$N_{q,n} = -\left[v_n(q) \cdot \nabla T\right] \tau_n(q) \frac{\partial N_{q,n}^0}{\partial T} + N_{q,n}^0. \tag{20}$$

and noting the definition $J = -\kappa \nabla T$, the expression of phonon thermal conductivity can be obtained as [49]:

$$\kappa(T) = \frac{1}{3}\left(\frac{k_B}{\hbar}\right) k_B T \sum_n \int \frac{x^2 e^x}{\left(e^x - 1\right)^2} f_n(x) v_n^2(x) \tau_n(x) dx, \tag{21}$$

where, $x = \hbar\omega / k_B T$, k_B, τ_n, and T are the Boltazmann constant, phonon relaxation time, and temperature, respectively.

There are many phonon scattering mechanisms in semiconductor materials relating the phonon relaxation time τ_n. Since this work focuses on the influence of surface/interface stress on phonon behavior and thermal conductivity in heterostructural nanofilm, the phonon boundary scattering mechanism is neglected based on the assumption of smooth boundaries. In the following analysis, Umklapp scattering rate τ_U, point defect scattering rate τ_M, and acoustic phonon-electron scattering rate τ_{ph-e} are considered; and the relaxation time follows Matthiessen rule, given as [45, 48, 49]

$$\tau_T^{-1} = \tau_U^{-1} + \tau_{ph-e}^{-1} + \tau_M^{-1}, \quad (22)$$

Here, the Umklaap scattering rate is given by

$$\frac{1}{\tau_U} = 2\gamma^2 \frac{k_B T}{\mu V_0} \frac{\omega^2}{\omega_D}, \quad (23)$$

where γ is the anharmonic parameter of Grunieisen, ω_D is Debye frequency, $V_0 = \sqrt{3}a^2 c/8$ is the monatomic volume with *a* and *c* being the lattice constants. The expression of point defect scattering rate is given by

$$\frac{1}{\tau_M} = \frac{V_0 \Gamma \omega^4}{4\pi V^3}, \quad (24)$$

where V is the phonon group velocity and Γ is the measure of scattering length. In the case of low doping density, the phonon-electron scattering relaxation time can be expressed as

$$\frac{1}{\tau_{ph-e}} = \sqrt{\frac{\pi m^* V^2}{2k_B T}} \exp\left(-\frac{\pi m^* V^2}{2k_B T}\right) \frac{n_e \varepsilon_1^2 \omega}{\rho V_e^2 k_B T}, \quad (25)$$

where V_e is the effective mass of a potential electron, n_e is the carrier density, ε_1 is the deformation potential, m^* is the electron effective mass, and ρ is the density. The parameters used in the following calculation are $\gamma = 0.74$, $\omega_D = 830K$, $\Gamma = 2.49\times10^{-2}$, $n_e = 2.3\times10^{19}\,\mathrm{cm}^{-3}$, $\varepsilon_1 = 10.1\mathrm{eV}$, and $m^* = 0.22m_e$,

where m_e is the electron mass [52-54].

3 Results and Discussion

3.1 Influence of surface/interface stress on phonon properties

In this section, we carry out numerical calculations for different GaN-based heterogeneous nanofilms to discuss the phonon properties under different surface/interface stresses. The elastic modulus of wurtzite GaN and AlN used in the calculation are shown in Table 1 [55, 56]. The equibiaxial surface stress can be tensile or compressive depending on the adhesion of the surface atom to its neighboring atoms. Hence, three typical surface/interface stresses are selected, namely, 5 N/m, -5 N/m, and zero stress. We compare four kinds of nanofilms with the thickness of 6 nm. They are the homogeneous GaN nanofilm, homogeneous AlN nanofilm, and GaN-based heterostructural nanofilms with the interlayer thicknesses of 3nm and 2nm, respectively.

Taking SH mode as an example, the influences of surface/interface stress on phonon properties are calculated. Figures 2 and 3 plot the dispersion relations of four kinds of nanofilms with different surface/interface stresses. Due to the spatial confinement effect on phonons in nanofilms, there are a set of curves for SH mode in figures 2 and 3. In Figs. 2(d) and 3(d) for the GaN and AlN naonfilms, respectively, the two oblique lines represent the dispersion relations of the bulk GaN and bulk AlN, respectively, and the other dispersion relation curves become closer to these two characteristic lines with increasing the wave

vector. The results of heterostructural nanofilms also contain these characteristic lines, as shown in Figs. 2(a-c) and 3(a-c). With the increase of wave vector, the dispersion relation curves become closer to GaN characteristic line, belong to the GaN layer in the heterostructural films, and those closer to AlN characteristic line represent the modes from AlN layers. By comparing phonon dispersion curves under different surface/interface stresses in the figure, it can be observed that positive surface/interface stress increases phonon energy, and vice versa. When the phonon wave vector is at the truncation frequency (q=0), there is almost no influence of surface/interface stress on the phonon energy. With the increase of the wave vector, the influence of surface/interface stress becomes gradually more significant, which is the case for the four nanofilms studied. It is further noted that the effect of surface/interface stress in the heterostructural nanofilms is more significant than that in the homogenous nanofilms. This is because with the same thickness of the nanofilm, there are two additional interfaces in heterostructural nanofilms.

According to the dispersion curves, the phonon group velocity can be calculated as shown in figures 4 and 5. The group velocity of phonon is derived from dispersion relations, leading to that there exit a set of curves for group velocity of phonons in figures 4 and 5. In Figs. 4(d) and 5(d) for the GaN and AlN nanofilms respectively, the straight lines represent the phonon group velocity. It is noted that the phonon group velocity in GaN is much lower than that in AlN. Different from the homogeneous materials, the group velocity curves of the heterogeneous structures oscillate with *q*, as shown in Figs. 4(a-c) and 5(a-c). This is originated from the

thickness-dpendent elastic properties in heterostructural nanofilms, leading to the coupling effect of atomic vibrations. With the increase of wave vector, the group velocity curves converge to the group velocity lines of bulks. Further, one can note that the surface/interface stress significantly affects the phonon group velocity of the nanostructure. That is, the positive surface stress increases the phonon group velocity, and vice versa. The average group velocities of the four kinds of nanofilms under different surface/interface stresses are shown in Figure 6, which also shows that the phonon average group velocity increases with surface and interface stresses. One can also notice from Figs. 4-6 that the influences of surface/interface stresses on the phonon (average) group velocity of heterostructural nanofilms are more significant than of homogeneous nanofilms because of the interfaces.

The phonon DOS can also be calculated from Eq. (17) for various nanofilms. Figure 7 compares the phonon DOS of homogenous and heterostructural nanofilms with different surface/interfaces stresses. It is noted that with the increase of phonon energy, the DOS increases stepwise and then decreases after reaching a peak, which is caused by the quantum confinement effect. It can be found that the existence of surface/interface stress changes the peak value of DOS and the corresponding phonon energy. That is, the positive surface/interface stress reduces the peak value of DOS and makes the peak value appear in the region with higher phonon energy, and vice versa. Note that the effect of surface/interface stress on phonon DOS is opposite to that on phonon group velocity, because the phonon density of state is inversely proportional to the phonon group velocity.

3.2 Influence of surface/interface stress on phonon thermal conductivity

With the phonon dispersion relation, group velocity and DOS, the phonon thermal conductivity at different temperatures and under different surface/interface stresses can be numerically calculated based on Eq. (21). Suppose that the surface/interface stress varies from -10 N /m to 10 N/m, and all the surface/interface stresses in these surfaces and interfaces are in the same direction. When the temperature is 300K, the phonon thermal conductivities in SH mode of different nanofilms are shown in Fig. 8(a). As the surface/interface stress increases from negative to positive, the phonon thermal conductivity of the four nanostructures increases accordingly. Among them, the thermal conductivity of homogeneous AlN is the highest, while that of homogeneous GaN is the lowest. In the AS mode, the thermal conductivities of the heterostructural nanofilms and AlN nanofilm decrease with the increase of surface/interface stress as shown in Fig. 8(b), while only that of the GaN nanofilm, on the contrary, increases with the increase of surface/interface stress. When the surface/interface stress is larger, the upward trend is more obvious. The results in SA mode are plotted in Fig. 8(c), which shows that the phonon thermal conductivities in AS and SA modes have a similar trend with the change of surface/interface stress.

Note that with increasing the surface/interface stress, the stress-dependent thermal conductivity of GaN nanofilm is different from that of AlN nanofilm and heterostructural nanofilms in SA and AS modes, as shown in Fig. 8. Such a

phenomenon originates from the difference of effective elastic modulus $\bar{C}_{44}$ in GaN and AlN nanofilms. The dispersion relations for SA and AS modes are sensitive to $\bar{C}_{44}$ as indicated by Eq. (8). Since the elastic modulus C_{144} is negative in GaN but becomes positive in AlN as shown in Table 1, as a result the effective modulus $\bar{C}_{44}$ increases in GaN and decreases in AlN with surface/interfae stress. AlN layers are dominant in the heterostructured nanofilm, therefore, the stress dependence of thermal conductivity in AS and SA modes is similar in the AlN and heterostructured nanofilms.

The phonon thermal conductivity of GaN-based heterostructural nanofilms at 100K, 300K and 500K is further calculated and depicted in Fig. 9. For SH mode as shown in Fig. 9(a), the phonon thermal conductivity keeps increasing as the surface/interface stress increases from negative to positive magnitudes. Fig. 9(a) indicates that the stress dependence (i.e., the slops) of phonon thermal conductivity curves varies with temperature, i.e., the lower temperature results in the more significant dependence on surface/interface stress. Figs. 9(b) and 9(c) show the phonon thermal conductivities in AS and SA modes at different temperatures. The variation of thermal conductivity of heterostructural nanofilms at different temperatures is consistent with that in Figs. 8(b) and 8(c). With the surface/interface stress varied from -10 N/m to 10 N/m, the phonon thermal conductivity in SA and AS modes gradually decreases. One may also note that the influence of surface/interface stress on the thermal conductivity of SH mode is much more notable than those of SA and AS modes.

Finally, the temperature dependence of phonon thermal conductivity under different surface/interface stresses can also be obtained. Taking 5 N/m, 0 N/m, -5 N/m as examples, the calculation results for SH, SA and AS modes are shown in figure 10.With the increase of temperature, phonon thermal conductivities in the three modes rises first and then descends. The peaks of phonon thermal conductivity in the three modes occur at different temperatures, which are also affected by surface/interface stress. In Fig. 10, it is more clearly shown that the surface/interface stress has a more significant impact on the thermal conductivity in SH mode than those in SA and AS modes. While the temperature increases from the low temperature to the critical value of maximum conductivity, the influence of surface/interface stress becomes gradually more remarkable. With the further increase of temperature, the effect of surface/interface stress on thermal conductivity becomes gradually weaker.

4 Conclusion and Remarks

In summary, the effects of surface/interface stress on the phonon and thermal properties of GaN-based heterostructural nanofilms are investigated theoretically. Considering the influence of surface/interface stress on the elastic modulus, a modified elastic model is applied to analyze quantitatively the influence of surface/interface stress on phonon properties such as the phonon dispersion relation, group velocity, DOS, and on the phonon thermal conductivity of nanofilms. **Numerical results demonstrated that surface/interface stress can significantly change phonon properties and the phonon thermal conductivity of GaN-based**

nanofilms. With the surface/interface stress varied from negative to positive magnitude, the phonon thermal conductivity of the nanostructure increases in SH mode but deceases in AS and SA modes, **owing to the different effect of surface/interface stress on the effective modulus.** It is further found that the phonon thermal conductivity in nanofilms is affected by the surface/interface stress and temperature. These results will be helpful to optimize phonon properties and phonon thermal conductivity of heterostructural nanofilms through surface/interface engineering, and provide the theoretical basis for the rational design of GaN-based electronic devices with excellent performance in the future.

It should be pointed out that the proposed theoretical description of the phonon properties and thermal conductivity of nanofilms are applicable to the case that the phonons spatially confined in nanostructures. The theoretical model does not involve phonon scattering at surfaces and interfaces, which could affect the phonon transport along the in-plane and transversal directions, as shown in Ref. [57-60]. Therefore, our model could be further developed to involve the influence of surface/interface phonon scattering. In addition, our work has shown the effects of surface/interface stress on thermal conductivity in different phonon modes. Therefore, the exact heat transfer behavior in GaN-based nanoelectronic devices is also an important topic for further investigation.

Acknowledgement

This research is supported by the National Natural Science Foundation of China

(Grant nos. 11772294, 11621062, 11302189), and the Fundamental Research Funds for the Central Universities (Grant no. 2017QNA4031).

Reference

[1] F. Weigend, F. Evers, J. Weissmüller, Structural Relaxation in Charged Metal Surfaces and Cluster Ions. Small 2, 1497-1503 (2006).

[2] C.Q. Sun, Thermo-mechanical behavior of low-dimensional systems: The local bond average approach. Prog. Mater. Sci. 54, 179-307 (2009).

[3] L.M.C. Sagis, Dynamic properties of interfaces in softer matter: Experiments and theory. Rev. Mod. Phys. 83, 1367-1403 (2011).

[4] A. Javili, A. Mcbride, P. Steinmann, Thermomechanics of Solids With Lower-Dimensional Energetics: On the Importance of Surface, Interface, and Curve Structures at the Nanoscale. A Unifying Review. Appl. Mech. Rev. 65, 010802 (2013).

[5] R. Dingreville, J. Qu, M. Cherkaoui, Surface free energy and its effect on the elastic behavior of nano-sized particles, wires and films. J. Mech. Phys. Solids 38, 1827-1854 (2005).

[6] P. Sharma, L.T. Wheeler, Size-dependent elastic state of ellipsoidal nano-inclusions incorporating surface/interface tension. J. Appl. Mech. 74, 447-454 (2007).

[7] J.X. Wang, Z.P. Huang, H.L. Duan, S.W. Yu, X.Q. Feng, G.F. Wang, W.X. Zhang, T.J. Wang, Surface stress effect in mechanics of nanostructured materials. Acta

Mech. Solida Sinica 24, 52-82 (2011).

[8] Q. Chen, G.N. Wang, M.J. Pindera, Homogenization and localization of nanoporous composites - A critical review and new developments. Compos. Part B-Eng 155, 329-368 (2018).

[9] M. Karimi, A.R. Shahidi, Comparing magnitudes of surface energy stress in synchronous and asynchronous bending/buckling analysis of slanting double-layer METE nanoplates. Appl. Phys. A 125, 154 (2019).

[10] A.I. Rusanov, Surface thermodynamics revisited. Surf. Sci. Rep. 58, 111-239 (2005).

[11] F. Fischer, T. Waitz, D. Vollath, N.K. Simha, On the role of surface energy and surface stress in phase-transforming nanoparticles. Prog. Mater. Sci. 53, 481-527 (2008).

[12] F. Frost, B. Ziberi, A. Schindler, B. Rauschenbach, Surface engineering with ion beams: from self-organized nanostructures to ultra-smooth surfaces. Appl. Phys. A 91, 551-559 (2008).

[13] I. Ferain, C.A. Colinge, J.P. Colinge, Multigate transistors as the future of classical metal-oxide-semiconductor field-effect transistors. Nature 479, 310-316 (2011).

[14] X. Wu, F. Fei, Z. Chen, W. Su, Z. Cui, A new nanocomposite dielectric ink and its application in printed thin-film transistors. Compos. Sci. Tech. 94, 117-122 (2014).

[15] Y. Guo, M. Wang, Phonon hydrodynamics and its applications in nanoscale heat

transport. Phys. Rep. 595, 1-44 (2015).

[16] F. Nasri, M.F.B. Aissa, H. Belmabrouk, Nanoheat conduction performance of black phosphorus field-effect transistor. IEEE T. Electron. Dev. 64, 2765-2769 (2017).

[17] H. Rezgui, F. Nasri, M.F.B. Aissa, H. Belmabrouk, A.A. Guizani, Modeling thermal performance of nano-gnrfet transistors using ballistic-diffusive equation. IEEE T. Electron. Dev. 65, 1611-1616 (2018).

[18] L.L. Zhu, X.J. Zheng, Influence of interface energy and grain boundary on the elastic modulus of nanocrystalline materials. Acta Mech. 213, 223-234 (2010).

[19] X. Gao, Z. Huang, J. Qu, D.N. Fang, A curvature-dependent interfacial energy-based interface stress theory and its applications to nano-structured materials:(I) general theory. J. Mech. Phys. Solids 66, 59-77 (2014).

[20] F. Ebrahimi, M.R. Barati, Vibration analysis of viscoelastic inhomogeneous nanobeams incorporating surface and thermal effects. Appl. Phys. A 123, 5 (2017).

[21] M. Karimi, A.R. Shahidi, A general comparison the surface layer degree on the out-of-phase and in-phase vibration behavior of a skew double-layer magneto–electro–thermo-elastic nanoplate. Appl. Phys. A 125, 106 (2019).

[22] M.E. Gurtin, A.I. Murdoch, A continuum theory of elastic material surfaces. Arch. Ration. Mech. An. 57, 291-323 (1975).

[23] P. Sharma, S. Ganti, N. Bhate, Effect of surfaces on the size-dependent elastic state of nano-inhomogeneities. Appl. Phys. Lett. 82, 535-537 (2003).

[24] L.H. He, C.W. Lim, B.S. Wu, A continuum model for size-dependent deformation of elastic films of nano-scale thickness. Int. J. Solids Struct. 41, 847-857 (2004).

[25] C. Chen, Y. Shi, Y.S. Zhang, J. Zhu, Y.J. Yan, Size dependence of Young's modulus in ZnO nanowires. Phys. Rev. Lett. 96, 075505 (2006).

[26] W. Xu, H. Ma, S. Ji, H. Chen, Analytical effective elastic properties of particulate composites with soft interfaces around anisotropic particles. Compos. Sci. Tech. 129, 10-18 (2016)

[27] M. Karimi, A.R. Shahidi, Nonlocal, refined plate, and surface effects theories used to analyze free vibration of magnetoelectroelastic nanoplates under thermo-mechanical and shear loadings. Appl. Phys. A 123, 304 (2017).

[28] M. Karimi, H.R. Mirdamadi, A. R. Shahidi, Positive and negative surface effects on the buckling and vibration of rectangular nanoplates under biaxial and shear in-plane loadings based on nonlocal elasticity theory. J. Braz.Soc. Mech. Sci. 39, 1391-1404 (2017)

[29] M. Karimi, A.R. Shahidi, Buckling analysis of skew magneto-electro-thermo-elastic nanoplates considering surface energy layers and utilizing the Galerkin method. Appl. Phys. A 124, 681 (2018).

[30] M. Karimi, Rate of surface energy changes on the wave propagation analysis of METE nanoplates based on couple stress small-scale and nonlocal strain gradient theories. Mater. Res. Express 6, 085087 (2019).

[31] Z.Q. Wang, Y.P. Zhao, Z.P. Huang, The effects of surface tension on the elastic properties of nano structures. Int. J. Eng. Sci. 48, 140-150 (2010).

[32] R.E. Miller, V.B. Shenoy, Size-dependent elastic properties of nanosized structural elements. Nanotechnology 11, 139-147 (2000).

[33] M. Liangruksa, I.K. Puri, Lattice thermal conductivity of a silicon nanowire under surface stress. J. Appl. Phys. 109, 113501 (2011).

[34] J. Seyler, M.N. Wybourne, The effect of surface roughness on the phonon mean free path in narrow wires. J. Phys.: Condens. Mat. 2, 8853-8858 (1990).

[35] A.I. Hochbaum, R. Chen, R.D. Delgado, W. Liang, E.C. Garnett, M. Najarian, A. Majumdar, P.D. Yang, Enhanced thermoelectric performance of rough silicon nanowires. Nature 451, 163-167 (2008).

[36] L.L. Zhu and H.H. Ruan, Influence of prestress fields on the phonon thermal conductivity of GaN nanostructures. ASME J. Heat Transfer 136, 102402 (2014).

[37] H.N. Luo and L.L. Zhu, Effects of surface stress on the phonon properties in GaN nanofilms. ASME J. Appl. Mech. 82, 111002 (2015).

[38] L.L. Zhu and H.H. Ruan, Effects of pre-stress and surface stress on phonon thermal conductivity of rectangular Si nanowires. Appl. Phys. A 119, 253-263 (2015).

[39] L.L. Zhu and H.N. Luo, Phonon properties and thermal conductivity of GaN nanofilm under prestress and surface/interface stress. J. Alloy. Compd. 685, 619-625 (2016).

[40] A. Casian, I. Sur, H. Scherrer, Z. Dashevsky, Thermoelectric properties of n-type PbTe/Pb1-xEu xTe, quantum wells. Phys. Rev. B 61, 15965-15974 (2000).

[41] U.K. Mishra, P. Parikh, Y.F. Wu, AlGaN/GaN HEMTs-an overview of device

operation and applications. Proc. IEEE 90, 1022-1031 (2002).

[42] E. Kasper, D.J. Paul, Heterostructure Bipolar Transistors-HBTs (Berlin: Springer) (2005)

[43] A. Minj, D. Cavalcoli, A. Cavallini, Thermionic emission from the 2DEG assisted by image-charge-induced barrier lowering in AlInN/AlN/GaN heterostructures. Nanotechnology 23, 115701 (2012)

[44] C. Jiang, T. Liu, C. Du, X. Huang, M. Liu, Z. Zhao, L. Li, X. Pu, J. Zhai, W. Hu, Piezotronic effect tuned AlGaN/GaN high electron mobility transistor. Nanotechnology 28, 455203 (2017).

[45] J. Zou, X. Lange, C. Richardson, Lattice thermal conductivity of nanoscale AlN/GaN/AlN heterostructures: Effects of partial phonon spatial confinement. J. Appl. Phys. 100, 104309 (2006).

[46] N. Bannov, V.V. Aristov, V.V. Mitin, M.A. Stroscio, Electron relaxation times due to the deformation-potential interaction of electrons with confined acoustic phonons in a free-standing quantum well. Phys. Rev. B 51, 9930-9942 (1995).

[47] A. A. Balandin, Nanophononics: Phonon engineering in nanostructures and nanodevices. J. Nanosci. Nanotechnol. 5, 1015-1022 (2005).

[48] P, Martin. Z. Aksamija, E. Pop, U. Ravaioli, Impact of phonon-surface roughness scattering on thermal conductivity of thin Si nanowires. Phys. Rev. Lett. 102, 125503 (2009).

[49] G. Zhou and L.L. Li, Phonon thermal conductivity of GaN nanotubes. J. Appl. Phys. 112, 014317 (2012).

[50] M.H. Shokrani, M. Karimi, M.S. Tehrani, H.R. Mirdamadi, Buckling analysis of double-orthotropic nanoplates embedded in elastic media based on non-local two-variable refined plate theory using the GDQ method. J. Braz. Soc. Mech. Sci. 38, 2589-2606 (2016).

[51] M. Karimi, A.R. Shahidi, Thermo-mechanical vibration, buckling, and bending of orthotropic graphene sheets based on nonlocal two-variable refined plate theory using finite difference method considering surface energy effects. P. I. Mech. Eng. L: J. Nanomater. Nanoeng. Nanosys. 231, 111-130 (2017).

[52] E.K. Sichel, J.I. Pankove, Thermal Conductivity of GaN, 25–360 K. J. Phys. Chem. Solids, 38, 330 (1977).

[53] A. Witek, Some aspects of thermal conductivity of isotopically pure diamond-a comparison with nitrides. Diamond Relat. Mater. 7, 962-964 (1998).

[54] C. Guthy, C.-Y. Nam, and J. E. Fischer, Unusually low thermal conductivity of gallium nitride nanowires. J. Appl. Phys. 103, 064319 (2008).

[55] S.P. Łepkowski, Nonlinear elasticity in III-N compounds: ab initio calculations. Phys. Rev. B 72, 245201 (2005).

[56] S.P. Łepkowski, I. Gorczyca, Ab initio study of elastic constants in InxGa1−xNand InxAl1-xNwurtzite alloys. Phys. Rev. B 83, 203201 (2011).

[57] G. Chen, Thermal conductivity and ballistic-phonon transport in the cross-plane direction of superlattices. Phys. Rev. B 57, 14958-14973 (1998).

[58] X.J. Zheng, L.L. Zhu, Y.H. Zhou, Q.J. Zhang, Impact of grain sizes on phonon thermal conductivity of bulk thermoelectric materials. Appl. Phys. Lett. 87, 242101-242103 (2005).

[59] Y. Hou, L.L. Zhu, Influence of surface scattering on the thermal properties of spatially confined GaN nanofilm. Chin. Phys. B 25, 086502 (2016).

[60] L.L. Zhu, X.Y. Tang, J.C. Wang, Y. Hou, Modeling phonon thermal conductivity in spatially confined GaN nanofilms under stress fields and phonon surface scattering. AIP Adv. 9, 015024 (2019).

List of Captions

Table 1. Elastic modulus of AlN/GaN/AlN nanofilms used in simulations.

Figure 1. Schematical drawing for GaN-based heterostructural nanofilm.The dark part refers to GaN layer and the white parts refer to AlN layers.

Figure 2. The phonon dispersions of AlN/GaN/AlN(1.5nm/3nm/1.5nm) nanofilm and GaN nanofilm with different surface/interface stresses for SH mode.

Figure 3. The phonon dispersions of AlN/GaN/AlN(2nm/2nm/2nm) nanofilm and AlN nanofilm with different surface/interface stresses for SH mode.

Figure 4. The phonon group velocities as the function of wave vector for AlN/GaN/AlN(1.5nm/3nm/1.5nm) nanofilm and GaN nanofilm with different surface/interface stresses for SH mode.

Figure 5. The phonon group velocities as the function of wave vector for AlN/GaN/AlN(2nm/2nm/2nm) nanofilm and AlN nanofilm with different surface/interface stresses for SH mode.

Figure 6. The phonon average group velocities as the function of phonon energy for GaN-based heterostructural nanofilms, GaN nanofilm and AlN with different surface/interface stresses for SH mode.

Figure 7. The phonon densities of state as the function of phonon energy for GaN-based heterostructural nanofilms, GaN nanofilm and AlN with different surface/interface stresses for SH mode.

Figure 8. The phonon thermal conductivities of SH mode (a), AS mode (b) and SA (c) mode as the function of surface/interface stress for GaN-based heterostructural nanofilms, GaN nanofilm and AlN.

Figure 9. The phonon thermal conductivities of SH mode (a), AS mode (b) and SA (c) mode as the function of surface/interface stress for GaN-based heterostructural nanofilm with different temperatures.

Figure 10. The phonon thermal conductivities of SH mode (a), AS mode (b) and SA (c) mode as the function of temperature for GaN-based heterostructural nanofilm with different surface/interface stresses.

Table 1. Elastic modulus of AlN/GaN/AlN nanofilms used in simulations.

GaN	C11(GPa)	C13(GPa)	C55(GPa)	C111(GPa)	C123(GPa)
	252	129	148	-1213	-253
	C144(GPa)	C155(GPa)	C112(GPa)	C456(GPa)	ρ(kg/m³)
	-46	-606	-867	-49	6100
AlN	C11(GPa)	C13(GPa)	C55(GPa)	C111(GPa)	C123(GPa)
	282	149	179	-1073	-61
	C144(GPa)	C155(GPa)	C112(GPa)	C456(GPa)	ρ(kg/m³)
	57	-757	-965	-9	3235

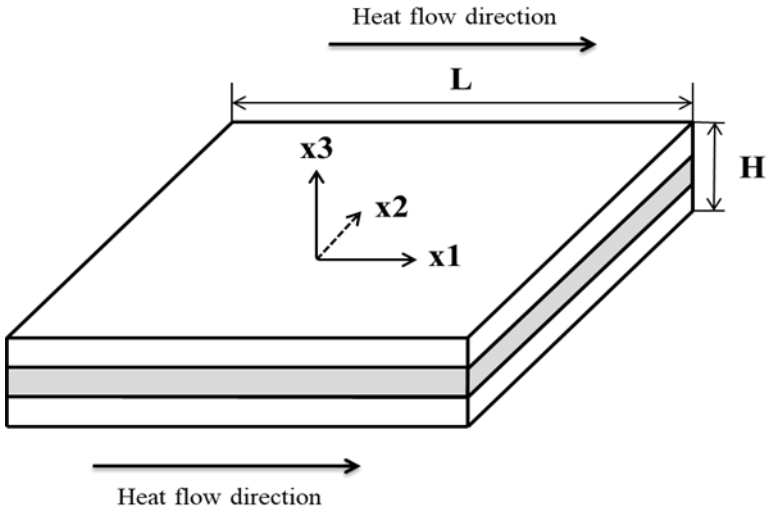

Figure 1. Schematical drawing for GaN-based heterostructural nanofilm.The dark part refers to GaN layer and the white parts refer to AlN layers.

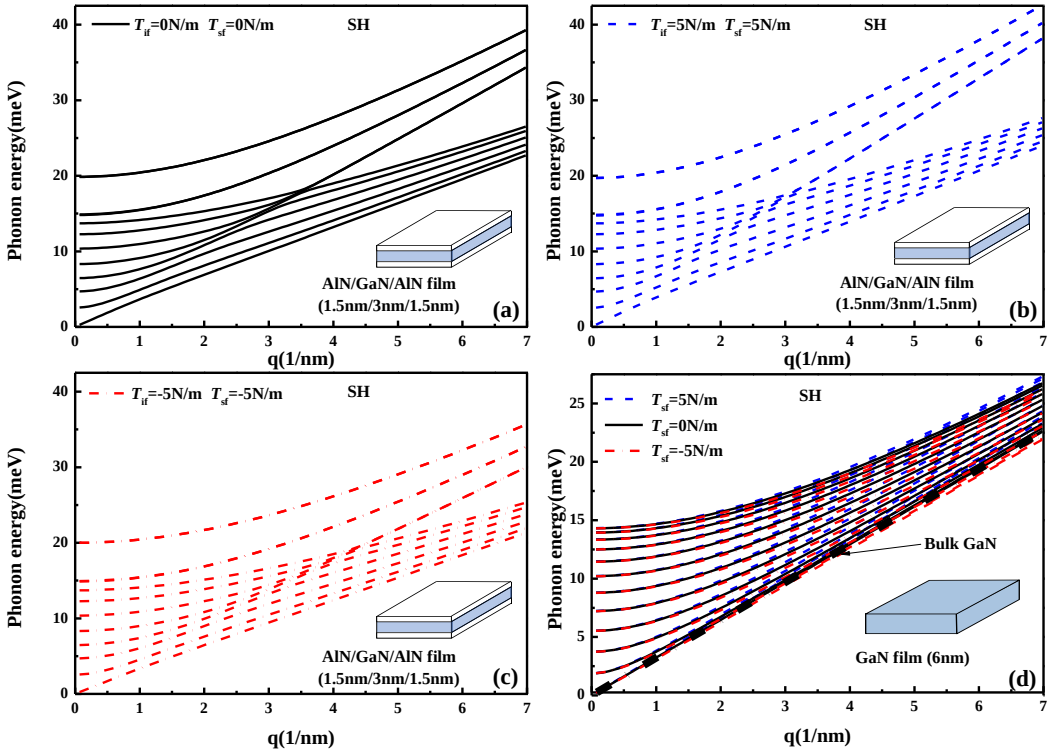

Figure 2. The phonon dispersions of AlN/GaN/AlN(1.5nm/3nm/1.5nm) nanofilm and GaN nanofilm with different surface/interface stresses for SH mode.

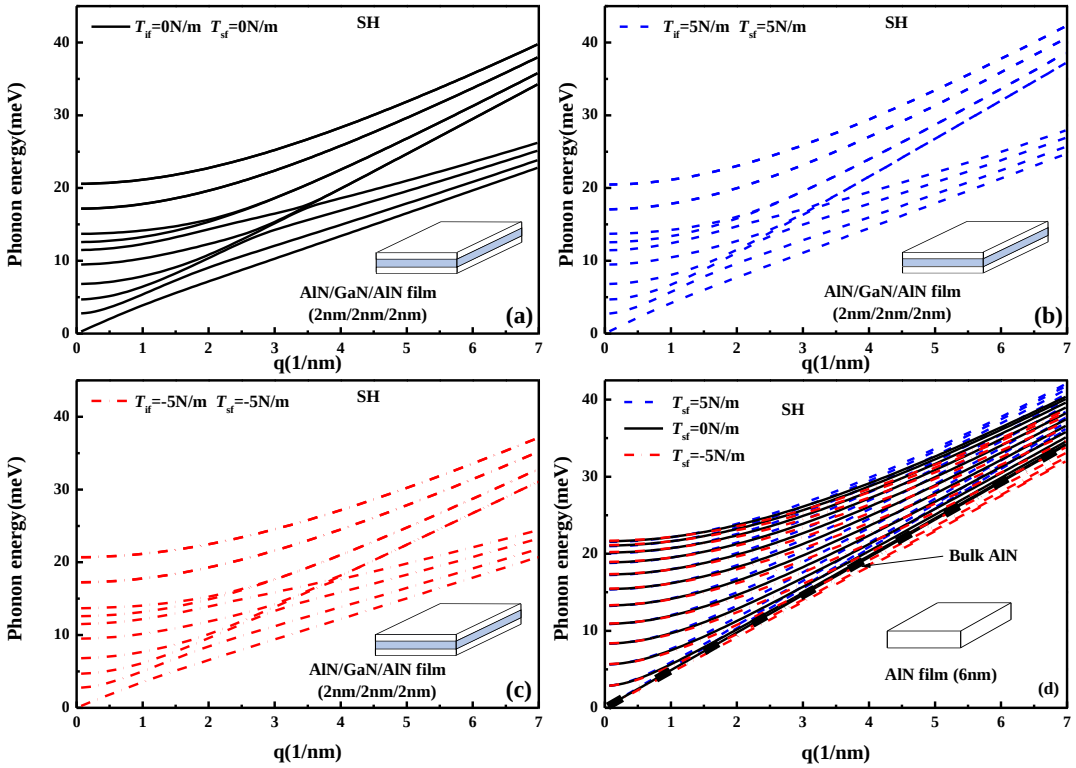

Figure 3. The phonon dispersions of AlN/GaN/AlN(2nm/2nm/2nm) nanofilm and AlN nanofilm with different surface/interface stresses for SH mode.

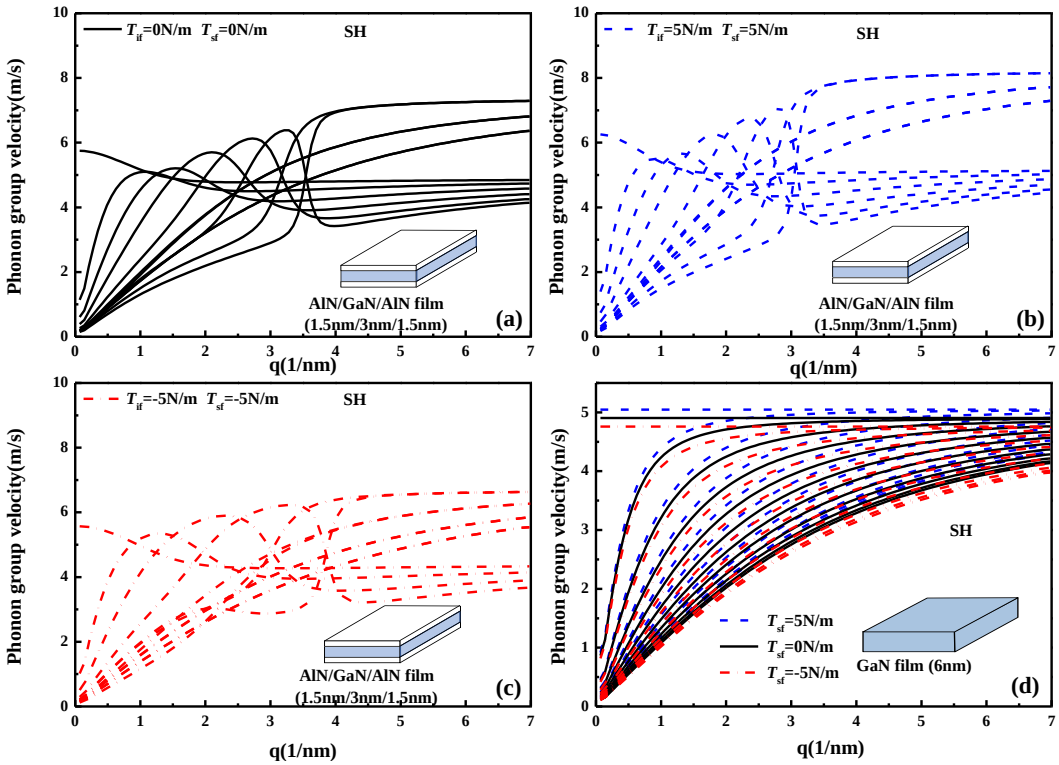

Figure 4. The phonon group velocities as the function of wave vector for AlN/GaN/AlN(1.5nm/3nm/1.5nm) nanofilm and GaN nanofilm with different surface/interface stresses for SH mode.

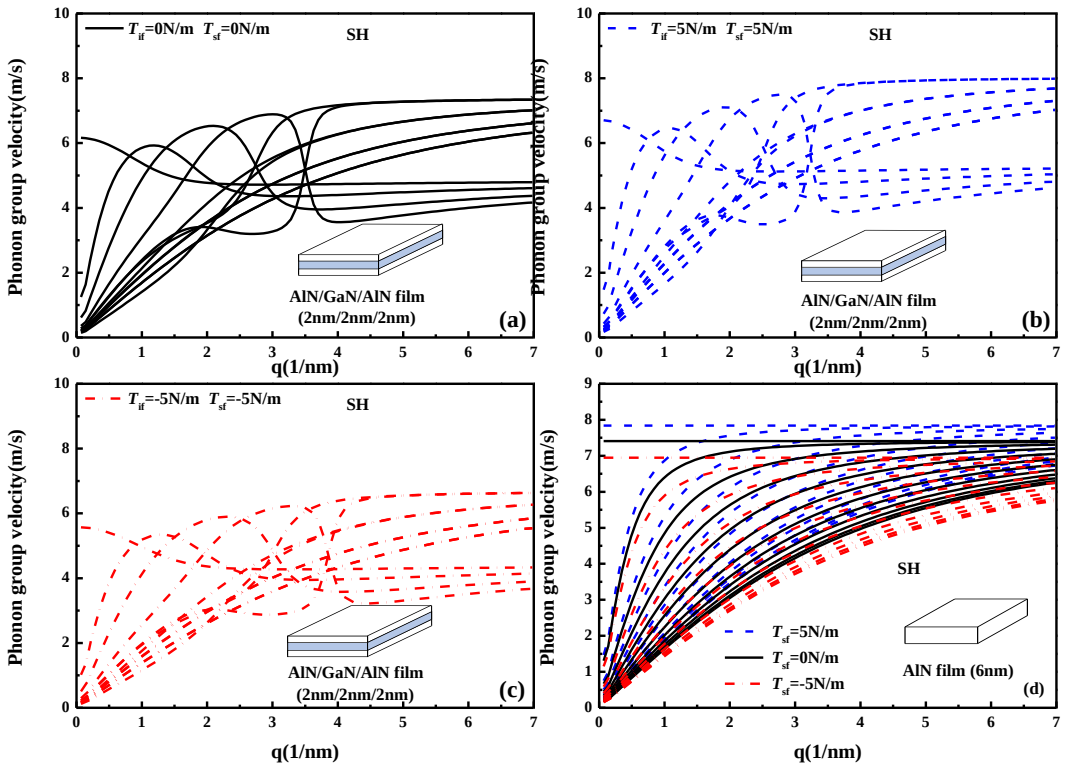

Figure 5. The phonon group velocities as the function of wave vector for AlN/GaN/AlN(2nm/2nm/2nm) nanofilm and AlN nanofilm with different surface/interface stresses for SH mode.

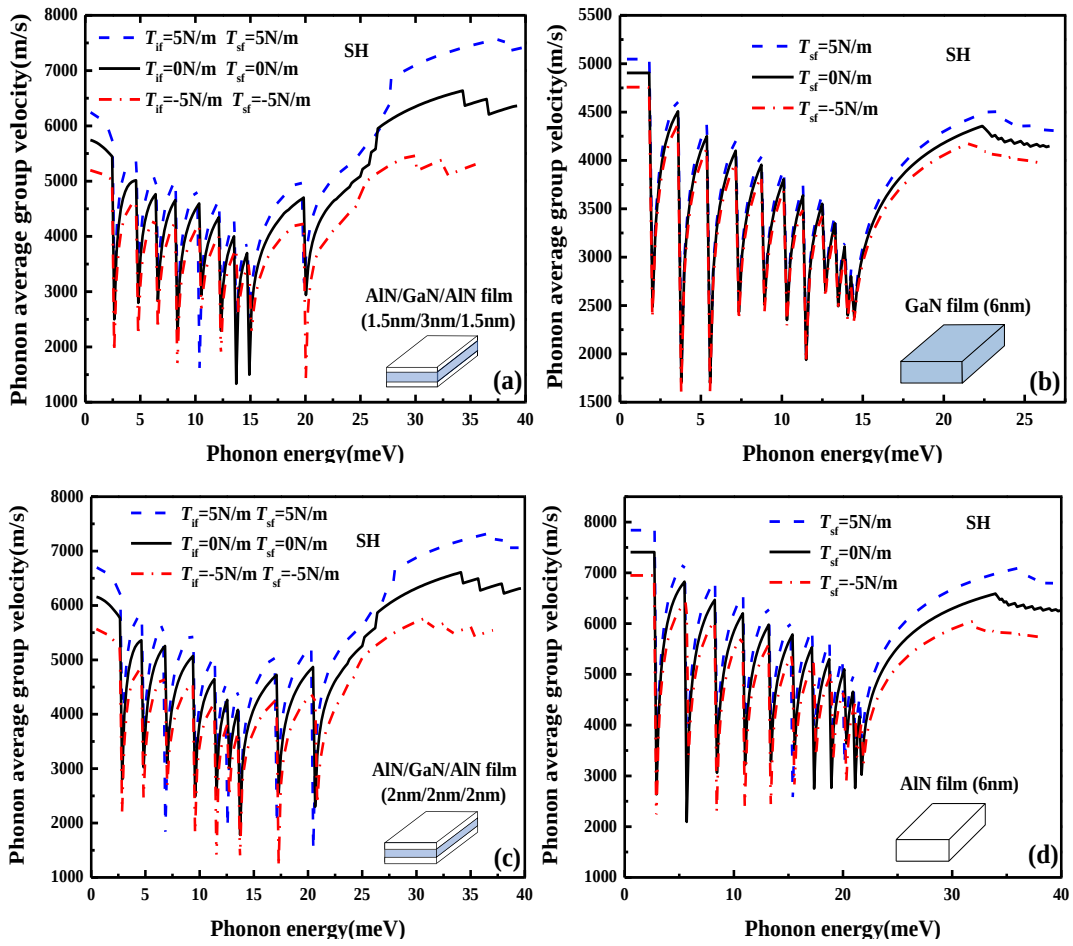

Figure 6. The phonon average group velocities as the function of phonon energy for AlN/GaN/AlN(2nm/2nm/2nm) nanofilm and AlN nanofilm with different surface/interface stresses for SH mode.

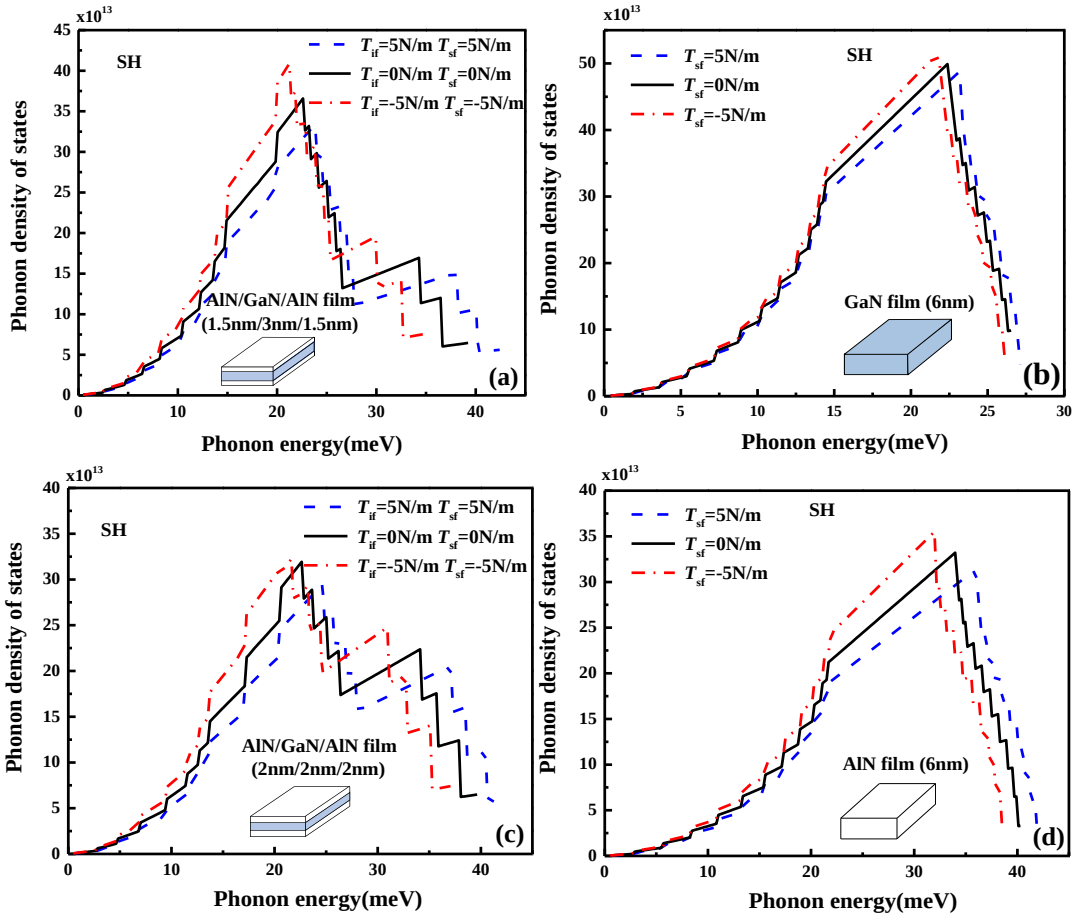

Figure 7. The phonon densities of state as the function of phonon energy for GaN-based heterostructural nanofilms, GaN nanofilm and AlN with different surface/interface stresses for SH mode.

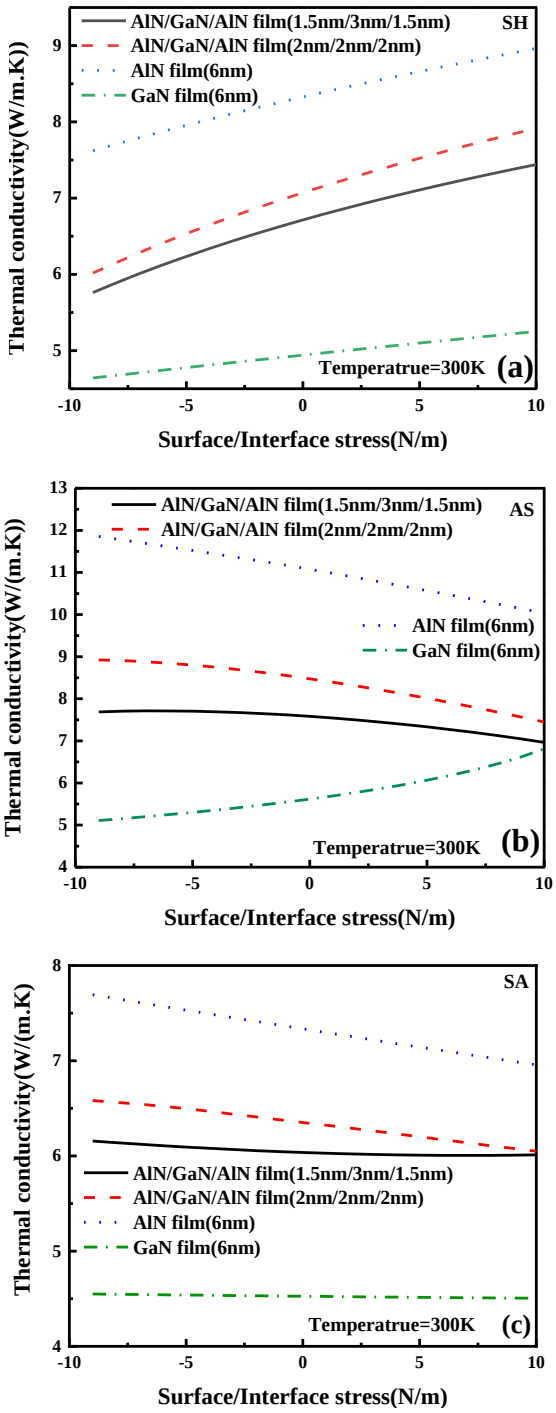

Figure 8. The phonon thermal conductivities of SH mode (a), AS mode (b) and SA (c) mode as the function of surface/interface stress for GaN-based heterostructural nanofilms, GaN nanofilm and AlN.

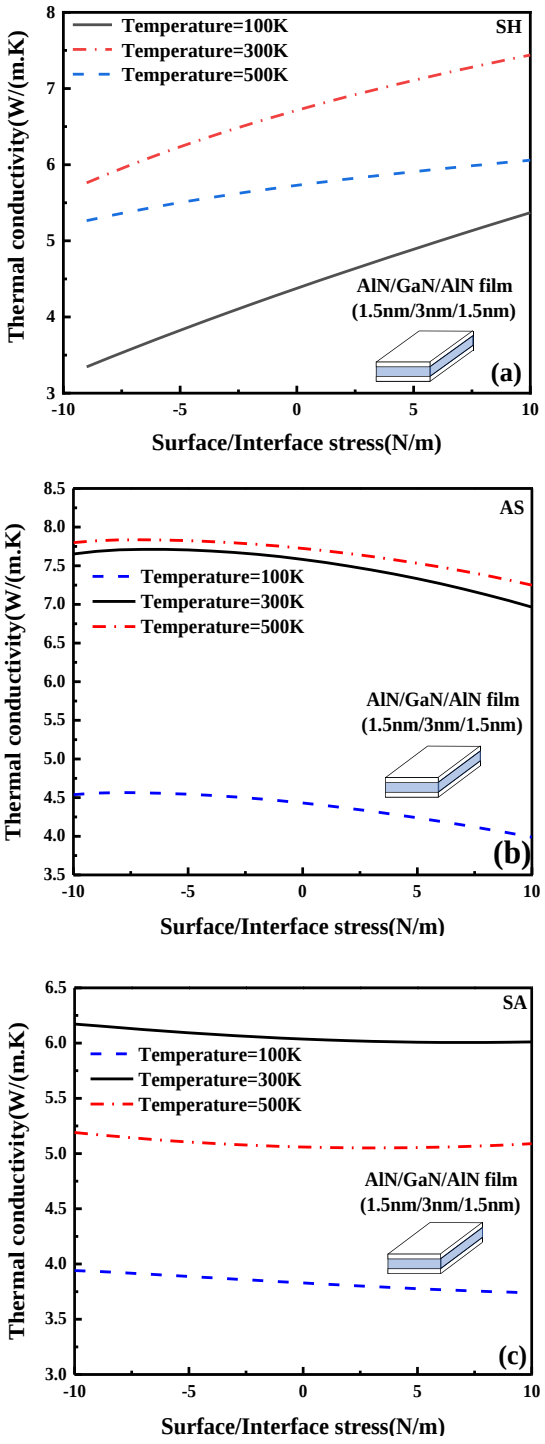

Figure 9. The phonon thermal conductivities of SH mode (a), AS mode (b) and SA (c) mode as the function of surface/interface stress for GaN-based heterostructural nanofilm with different temperatures.

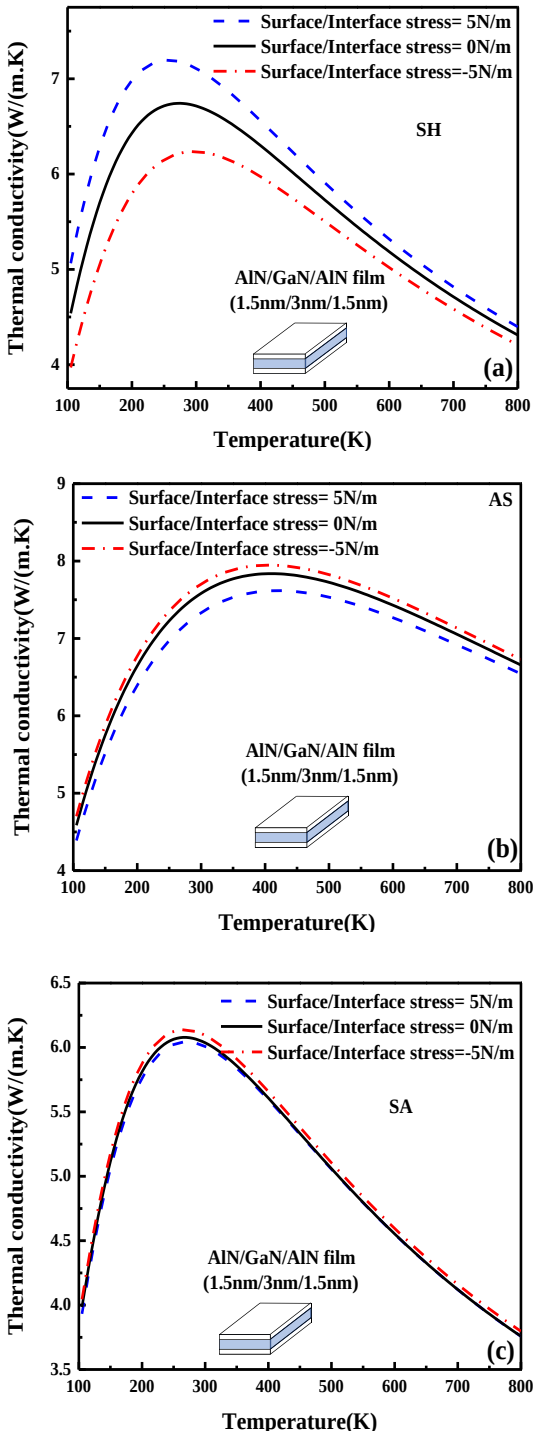

Figure 10. The phonon thermal conductivities of SH mode (a), AS mode (b) and SA (c) mode as the function of temperature for GaN-based heterostructural nanofilm with different surface/interface stresses.